

# Pressure-Induced Spin-State Crossovers in Six-Coordinate $\text{Fe}^{\text{II}}\text{L}_n\text{L}'_m(\text{NCS})_2$ Complexes with $\text{L} = \text{L}'$ and $\text{L} \neq \text{L}'$ : A XANES Investigation

Cécile Roux,<sup>1a,e</sup> Jacqueline Zarembowitch,<sup>\*,1a</sup> Jean-Paul Itié,<sup>1b,c</sup> Alain Polian,<sup>\*,1c</sup> and Michel Verdaguer<sup>1d</sup>

Laboratoire de Chimie Inorganique (CNRS, URA 420) and Laboratoire d'Utilisation du Rayonnement Electromagnétique (CNRS, MRES, CEA), Université Paris-Sud, 91405 Orsay, France, and Laboratoire de Physique des Milieux Condensés (CNRS, URA 782) and Laboratoire de Chimie des Métaux de Transition (CNRS, URA 419), Université P. et M. Curie, 4 Place Jussieu, 75252 Paris Cedex 05, France

Received June 7, 1995<sup>⊗</sup>

The pressure-induced iron(II) high-spin (HS)  $\rightarrow$  low-spin (LS) conversion has been investigated, by near-edge X-ray absorption (XANES) spectroscopy at room temperature, in a number of parent six-coordinate complexes of the type  $\text{FeL}_n\text{L}'_m(\text{NCS})_2$ , viz.  $\text{Fe}(\text{phen})_2(\text{NCS})_2$  form I (**1**) and form II (**2**),  $\text{Fe}(\text{py})_2\text{bpym}(\text{NCS})_2$  (**3**),  $\text{Fe}(\text{py})_2\text{phen}(\text{NCS})_2$  (**4**) and  $\text{Fe}(\text{py})_4(\text{NCS})_2$  (**5**), where phen = 1,10-phenanthroline, py = pyridine, and bpym = 2,2'-bipyrimidine. The spectra of the two spin isomers are interpreted. For compounds **1–4**, known to exhibit thermally-induced spin transitions,  $n_{\text{LS}}$  vs  $P$  plots ( $n_{\text{LS}}$  = LS fraction,  $P$  = pressure) are centered around  $P_c$  = 0.80 (**1**), 0.65 (**2**), 1.00 (**3**) and 1.55 (**4**) GPa. For **5**, which retains the HS form at any temperature under atmospheric pressure, the  $P_c$  value is much higher than the previous ones, lying in the range 5–7 GPa. After pressure was released, the spectra were found to be quite similar to those obtained before pressure was applied. The  $P_c$  values of **1–4** were analyzed in terms of spin-transition temperatures ( $T_c$ ), entropy ( $\Delta S$ ) and crystal volume ( $\Delta V_{\text{SC}}$ ) variations associated with the spin change, crystal structures, and volumic compressibility coefficients ( $k_v$ ), insofar as these data were available. The alteration of the spin-conversion development, when subjecting a compound (here **2**) several times to increasing then to decreasing pressures, was ascribed to a progressive decrease in the number of crystal defects (vacancies in particular).

## Introduction

High-spin (HS) state  $\leftrightarrow$  low-spin (LS) state crossovers, in transition-metal complexes, are known to be accompanied by a molecular reorganization, mainly consisting of a variation of metal–ligand distances ( $\Delta R$ ), and hence by an alteration of the unit-cell volume ( $\Delta V_{\text{SC}}$ ). It follows that pressure is a pertinent control parameter to trigger the spin change.

Most of the pressure-induced spin crossovers reported to date are related to iron(II) complexes (as examples, see refs 2 and 3 and the references given in ref 4), and several theoretical models were proposed to account for the experimental data.<sup>5–7</sup> The other papers are mainly devoted to cobalt(II) complexes.<sup>4,8,9</sup> Moreover, the first high-pressure single-crystal X-ray diffraction study of a spin-crossover system was recently reported.<sup>10–12</sup>

Finally, it should be noted that the combined effects of pressure and temperature have been the subject of a number of investigations.<sup>8,13–16</sup>

As first part of the work we have undertaken to specify the nature and the efficiency of the parameters governing the characteristics of pressure-induced spin crossovers (transition pressure, cooperativity, reversibility, ...) in  $d^4$  to  $d^7$  transition-metal complexes, we previously investigated a family of cobalt(II) compounds.<sup>4</sup> In the present paper, we report and discuss the data related to five parent six-coordinate iron(II) complexes. These species, which comply with the general formula  $\text{FeL}_m\text{L}'_n(\text{NCS})_2$  where L and L' represent different or identical ligands, are the following:<sup>17</sup>  $\text{Fe}(\text{phen})_2(\text{NCS})_2$ , the two crystalline forms<sup>18</sup> of which (form I = **1**, form II = **2**) were examined,  $\text{Fe}(\text{py})_2\text{bpym}(\text{NCS})_2$  (**3**),  $\text{Fe}(\text{py})_2\text{phen}(\text{NCS})_2$  (**4**), and  $\text{Fe}(\text{py})_4(\text{NCS})_2$  (**5**). Compounds **3–4** and **1–2** can be considered as derivatives of compound **5**, obtained by replacing 2 or 4 pyridine entities, respectively, by 1 or 2 bidentate ligands.

The choice of these complexes were dictated by several factors: (a) Their magnetic behaviors at variable temperatures are different, **1–2**<sup>18</sup> and **3–4**<sup>19</sup> exhibiting spin transitions whereas **5** retains the high-spin state.<sup>21</sup> (b) The enthalpies and

- <sup>⊗</sup> Abstract published in *Advance ACS Abstracts*, December 15, 1995.
- (1) (a) Laboratoire de Chimie Inorganique, Université Paris-Sud. (b) Laboratoire d'Utilisation du Rayonnement Electromagnétique, Université Paris-Sud. (c) Laboratoire de Physique des Milieux Condensés, Université P. et M. Curie. (d) Laboratoire de Chimie des Métaux de Transition, Université P. et M. Curie. (e) Present address: Laboratoire de Chimie de la Matière Condensée, Université P. et M. Curie, 4 Place Jussieu, 75252 Paris Cedex 05, France.
  - (2) Hammack, W. S.; Conti, A. J.; Hendrickson, D. N.; Drickamer, H. G. *J. Am. Chem. Soc.* **1989**, *111*, 1738.
  - (3) Konno, M.; Mikami-Kido, M. *Bull. Chem. Soc. Jpn.* **1991**, *64*, 339.
  - (4) Roux, C.; Zarembowitch, J.; Itié, J.-P.; Verdaguer, M.; Dartyge, E.; Fontaine A.; Tolentino, H. *Inorg. Chem.* **1991**, *30*, 3174.
  - (5) Slichter, C. P.; Drickamer, H. G. *J. Chem. Phys.* **1972**, *56*, 2142.
  - (6) Kambara, T. *J. Phys. Soc. Jpn.* **1981**, *50*, 2257.
  - (7) Sasaki, N.; Kambara, T. *J. Phys. Soc. Jpn.* **1982**, *51*, 1571.
  - (8) Sacconi, L.; Ferraro, J. R. *Inorg. Chim. Acta* **1974**, *9*, 49.
  - (9) Stephens, D. R.; Drickamer, H. G. *J. Chem. Phys.* **1961**, *35*, 429.
  - (10) Gaultier, J.; Granier, T.; Gallois, B.; Real, J. A.; Zarembowitch, J. *High Pressure Res.* **1991**, *7*, 336.
  - (11) Granier, T.; Gallois, B.; Suez-Panama, F.; Gaultier, J.; Real, J. A.; Zarembowitch, J. *Butll. Soc. Catalana Cien Fis., Quim. Mat.* **1992**, *13*, 293.

- (12) Granier, T.; Gallois, B.; Gaultier, J.; Real, J. A.; Zarembowitch, J. *Inorg. Chem.* **1993**, *32*, 5305.
- (13) Ferraro, J. R.; Takemoto, J. *Appl. Spectrosc.* **1974**, *28*, 66.
- (14) Usha, S.; Srinivasan, R. *Chem. Phys.* **1985**, *100*, 447.
- (15) König, E.; Ritter, G.; Waigel, J.; Goodwin, H. A. *J. Chem. Phys.* **1985**, *83*, 3055.
- (16) König, E.; Ritter, G.; Grünsteudel, H.; Dengler, J.; Nelson, J. *Inorg. Chem.* **1994**, *33*, 837.
- (17) Abbreviations: phen = 1,10-phenanthroline, py = pyridine, bpym = 2,2'-bipyrimidine, phy = 1,10-phenanthroline-2-carbaldehyde phenylhydrazone, and bpy = 2,2'-bipyridine.
- (18) Gallois, B.; Real, J. A.; Hauw, C.; Zarembowitch, J. *Inorg. Chem.* **1990**, *29*, 1152.

entropies of the transitions are known.<sup>19,20,22</sup> (c) Fe(phen)<sub>2</sub>(NCS)<sub>2</sub> was recently shown to present polymorphism,<sup>18</sup> **1** and **2** being the two identified crystalline forms. (d) The X-ray diffraction structures of **2**,<sup>18</sup> **3**,<sup>19</sup> **4**,<sup>23</sup> and **5**<sup>19,24</sup> at room temperature and of **2** at 130 K<sup>18</sup> have been determined, under atmospheric pressure ( $P_{\text{atm}}$ ). (e) The X-ray diffraction structure of a single crystal of **2** subjected to a pressure of 1 GPa (10 kbar) was just reported, together with the pressure-dependence of the unit cell parameters of this form.<sup>12</sup> (f) Fe(phen)<sub>2</sub>(NCS)<sub>2</sub> is the spin-crossover compound whose behavior under the effect of pressure has been most investigated, but the relevant data reveal inconsistencies and the polymorphism of this species was not yet detected when these studies were published.

The spin conversion was followed, at room temperature, using the near-edge structures of X-ray absorption (XANES) spectra. These structures are quite appropriate for such a study, since they depend on the spin-state of the metal ion through metal-ligand distances. Samples were examined in a diamond-anvil cell, designed for X-ray absorption experiments, allowing pressures up to  $\approx 15$  GPa to be applied.

### Experimental Section

**Syntheses.** All the syntheses were carried out under an argon atmosphere, and solvents were deoxygenated before use.

Compound **1** was prepared by extracting one 1,10-phenanthroline group from [Fe(phen)<sub>3</sub>](NCS)<sub>2</sub>·H<sub>2</sub>O with acetone in a soxhlet apparatus,<sup>25</sup> 3 weeks being required for the extraction to be completed. Crystals of **2** were obtained by the slow diffusion procedure previously reported.<sup>18</sup> The syntheses of **3** and **4** were conducted as described by Claude et al.<sup>19</sup> and by Herber,<sup>26</sup> respectively. **5** was prepared by using a method derived from that reported by Erickson and Sutin:<sup>27</sup> to an aqueous solution (60 mL) containing 3.93 mg (0.01 mol) of (NH<sub>4</sub>)<sub>2</sub>Fe(SO<sub>4</sub>)<sub>2</sub>·6H<sub>2</sub>O and 30 mg of ascorbic acid were gradually added 4 mL of pyridine and then 20 mL of an aqueous solution containing 1.6 g (0.02 mol) of ammonium thiocyanate. The mixture was stirred for 1 h at 0 °C. The yellow precipitate was filtered off at 0 °C, washed with 10 mL of an ethanol (27 mL)/pyridine (3 mL) solution (three times), with hot water, then with acetone, and dried for 2 days under an argon stream.

**High-Pressure System.** A Block-and-Piermarini diamond-anvil cell,<sup>28a</sup> the characteristics of which were reported in an earlier paper,<sup>4</sup> was used to apply high pressures to the samples. The pressure-transmitting medium was silicon oil, which allows nearly hydrostatic conditions to be obtained up to  $\approx 5$  GPa. Above this pressure, oil freezing prevents these conditions from continuing. Pressure calibration was performed by using the ruby fluorescence linear scale.<sup>28b</sup> The uncertainty on the values thus determined is less than 0.1 GPa below  $\approx 5$  GPa.

**X-ray Absorption Data Recording and Processing.** Room temperature X-ray absorption measurements were carried out at the energy dispersive EXAFS station of the LURE (Paris-Sud University).<sup>29,30</sup>

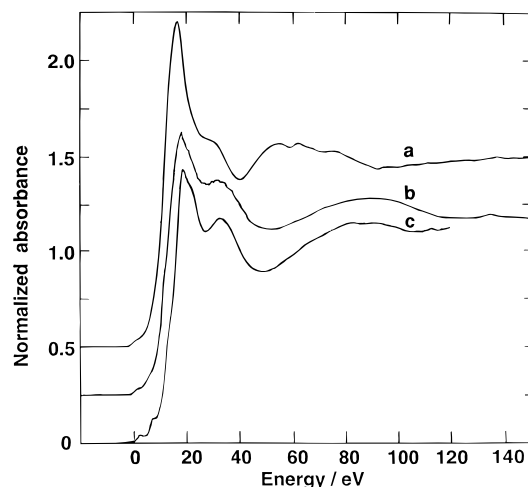


**Figure 1.** XANES spectra obtained for **1** under  $P_{\text{atm}}$  (a) and 1.7 GPa (b) at room temperature and at 77 K under  $P_{\text{atm}}$  (c). For clarity, spectra b and a were shifted upward by 0.25 and 0.50 eV, respectively.

Experimental details were given elsewhere.<sup>4</sup> Because of the strong absorption of the diamonds and the limited sample thickness, the data collection time for one spectrum was taken as 35–60 s depending on the sample, and 32 spectra were added for each applied pressure in order to increase the statistics. The experimental resolution, with a Si(111) polychromator, was evaluated at  $\approx 1.5$  eV and the width of the core hole at  $\approx 1.0$  eV. The data reproducibility was better than 0.5 eV. At the iron K-edge (7112 eV), used for the experiments, the energy band-pass allowed by the high-pressure cell was limited to ca. 200 eV, which restricted the reliable part of the spectra to the XANES range. Data processing has been discussed elsewhere.<sup>31,32</sup> For all the spectra, the energy origin was taken as 7112 eV and the absorbance was normalized at 1 at the atomic background.

### Results

For compound **1**, the HS-to-LS transformation was proven to be quasi-complete at high pressure, taking into account the close similarity (see Figure 1) of the spectra obtained at room temperature under a pressure of 1.7 GPa, and at 77 K under atmospheric pressure.<sup>33,34</sup> The latter can be effectively considered typical of the LS form, as variable-temperature magnetic measurements carried out on **1** showed that the residual HS form at very low temperature is lower than 3%.<sup>18</sup> It should be noted that such similarity of the spectra is likely to indicate that the molecular structures of the LS species resulting from pressure-induced and thermally-induced spin conversions are very close to each other. This property was established by König et al.<sup>35</sup> in the case of [Fe(phy)<sub>2</sub>](BF<sub>4</sub>)<sub>2</sub>,<sup>17</sup> on the basis of the close agreement observed between the corresponding values of the Mössbauer parameters  $\Delta E_Q(^1A_1)$  and  $\delta_{\text{is}}(^1A_1)$  for the two phases. Moreover we have shown recently, from the single-crystal X-ray diffraction structures of the LS forms of **2** (i) at 130 K under  $P_{\text{atm}}$ <sup>18</sup> and (ii) under 1 GPa at room temperature,<sup>12</sup> that the molecular structures of these two forms were nearly similar: Fe–N distances and N–Fe–N angles were found to differ by only 0.030–0.004 Å and 1.5–0.1°, respectively; however, the unit cell volume is significantly smaller under 1 GPa (2068 Å<sup>3</sup>) than at 130 K (2219 Å<sup>3</sup>).

- (19) Claude, R.; Real, J. A.; Zarembowitch, J.; Kahn, O.; Ouahab, L.; Grandjean, D.; Boukhedaden, K.; Varret, F.; Dworkin, A. *Inorg. Chem.* **1990**, *29*, 4442.  
 (20) Sorai, M.; Seki, S. *J. Phys. Chem. Solids* **1974**, *35*, 555.  
 (21) Little, B. F.; Long, G. J. *Inorg. Chem.* **1978**, *17*, 3401.  
 (22) Martin, J.-P.; Dworkin, A.; Zarembowitch, J. Unpublished results.  
 (23) Gallois, B.; Real, J. A.; Zarembowitch, J. To be published.  
 (24) Sotofte, I.; Rasmussen, S. E. *Acta Chem. Scand.* **1967**, *21*, 2028.  
 (25) Madeja, K.; Wilke, W.; Schmidt, S. Z. *Anorg. Allg. Chem.* **1966**, *346*, 306. Ganguli, P.; Gülich, P.; Müller, E. W. *J. Chem. Soc., Dalton Trans.* **1981**, 441.  
 (26) Herber, R. H. *Inorg. Chem.* **1987**, *26*, 173.  
 (27) Erickson, N. E.; Sutin, N. *Inorg. Chem.* **1966**, *5*, 1834.  
 (28) (a) Piermarini, G. J.; Block, S. *Rev. Sci. Instrum.* **1975**, *46*, 973. (b) Forman, R. A.; Piermarini, G. J.; Barnett, J. D.; Block, S. *Science* **1972**, *176*, 284.  
 (29) Tolentino, H.; Dartyge, E.; Fontaine, A.; Tourillon, G. *Applied Crystallogr.* **1988**, *21*, 15.  
 (30) Tolentino, H.; Baudelet, F.; Dartyge, E.; Fontaine, A.; Léna, A.; Tourillon, G. *Nucl. Instrum. Methods Phys. Res.* **1990**, *A289*, 307.

- (31) Polian, A.; Itié, J.-P.; Dartyge, E.; Fontaine, A.; Tourillon, G. *Phys. Rev.* **1989**, *B39*, 3369.  
 (32) Itié, J.-P.; Polian, A.; Jauberthie-Carillon, C.; Dartyge, E.; Fontaine, A.; Tolentino, H.; Tourillon, G. *Phys. Rev.* **1989**, *B40*, 9709.  
 (33) Cartier, C.; Thuéry, P.; Verdagner, M.; Zarembowitch, J.; Michalowicz, A. *J. Phys. C8*, **1986**, *47*, 563.  
 (34) Cartier, C. Thesis, Université Paris-Sud, 1988.  
 (35) König, E.; Ritter, G.; Kulshreshtha, S. K.; Waigel, J.; Goodwin, H. A. *Inorg. Chem.* **1984**, *23*, 1896.

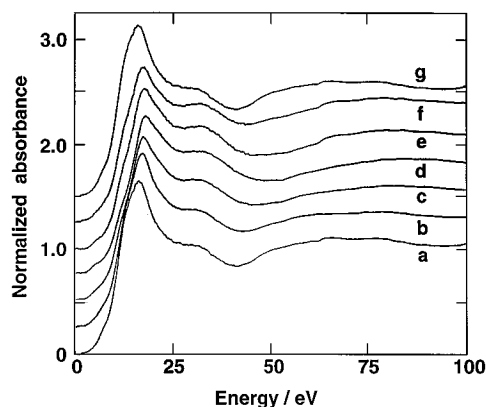


**Figure 2.** Selected XANES spectra obtained for **2** at room temperature under the following increasing then decreasing pressures:  $P_{\text{atm}}$  (a), 0.68 GPa (b), 0.87 GPa (c), 1.50 GPa (d), 0.73 GPa (e), 0.39 GPa (f), and  $P_{\text{atm}}$  (g). For clarity, each spectrum was shifted upward by 0.25 eV with regard to the preceding one.

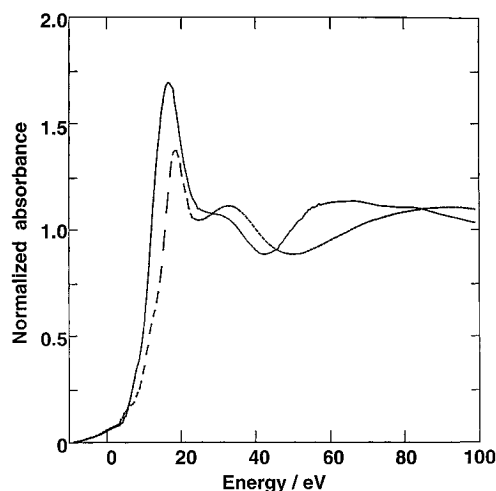


**Figure 3.** XANES spectra of **3** under  $P_{\text{atm}}$  (—) and 1.8 GPa (---) at room temperature.

By analogy with compound **1**, the pressure-induced HS-to-LS conversions exhibited by compounds **2–5** were assumed to be complete. This approximation is supported by the fact that the high-pressure spectra of all these species closely resemble each other, as can be seen in Figures 1–5. These Figures also show the spectra of the HS forms (at  $P = P_{\text{atm}}$ ) of **1–5**. In addition, Figure 2 represents a selection of the XANES spectra obtained for **2**, first at increasing then at decreasing pressures. It should be noted that, for all compounds, the spectra obtained at  $P_{\text{atm}}$  before and after the application of pressure are quite similar (as an example, see Figure 2), which is indicative of the reversibility of the spin conversion under the effect of pressure.

Taking the iron K-edge energy 7112 eV as the origin, the main XANES features characteristic of the HS (LS) species are the following (for each of them, we give the energy distribution in the spectra of complexes **1–5**): a strong absorption (white line) at 15.5–16.3 (17.3–18.7) eV, with shoulders at  $\sim 6$ –8 and  $\sim 12$ –13 ( $\sim 2$ –5 and  $\sim 10$ –12) eV, a medium intensity structure at 26–32 (26–32) eV and a pre-edge peak of low intensity at 0.1–1.9 eV (0.2–1.4 eV, observed only in the spectra of compounds **1**, **2**, and **4**). The white line is narrower and less intense for the LS forms than for the HS forms, while the structure at  $\approx 30$  eV is stronger. The spectra are completed by the first EXAFS oscillation, which spreads over  $\approx 60$  eV, and is shifted toward higher energies upon the HS-to-LS

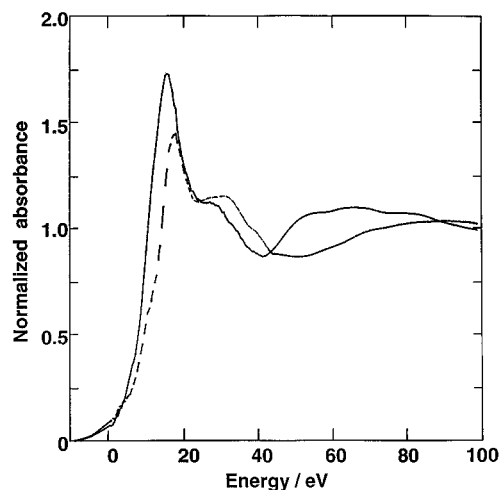


**Figure 4.** XANES spectra of **4** under  $P_{\text{atm}}$  (—) and 2.9 GPa (---) at room temperature.

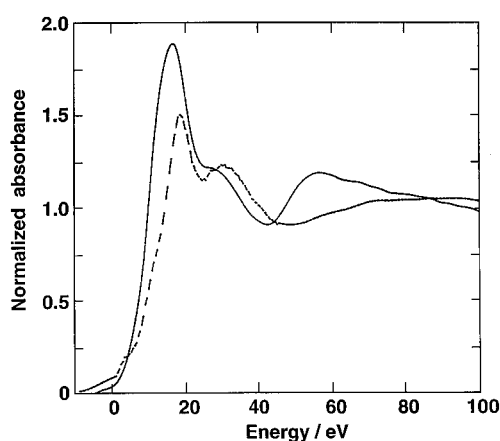


**Figure 5.** XANES spectra of **5** under  $P_{\text{atm}}$  (—) and 7.9 GPa (---) at room temperature.

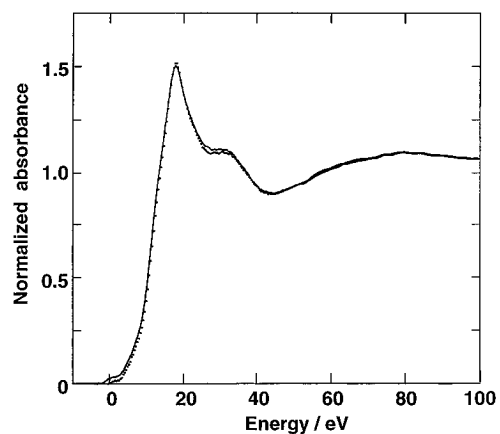


**Figure 6.** Comparison of the experimental spectrum obtained for **2** under 0.73 GPa (---) with the spectrum simulated for  $n_{\text{LS}} = 0.65$  (—).

conversion as a consequence of the shortening of metal-ligand distances.

Each spectrum, at a given pressure  $P$ , was simulated using a linear combination of the two spectra assumed to be those of the pure HS ( $n_{\text{LS}} = 0$ ) and LS ( $n_{\text{LS}} = 1$ ) species, which enabled the determination of the LS fraction  $n_{\text{LS}}$  at  $P$ . The agreement found between the experimental and calculated data is illustrated in Figure 6, and Figure 7 shows the spectra of **2** corresponding to different  $n_{\text{LS}}$  values.

The variation of  $n_{\text{LS}}$  as a function of  $P$  for compounds **1–4** is given in Figure 8. Regarding compound **5**, we only know

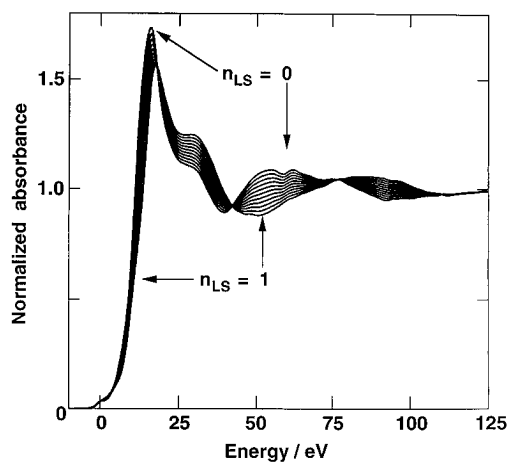


**Figure 7.** Simulated spectra of **2** for various values of the LS fraction ( $n_{LS} = 0.1, 0.2, \dots, 0.9$ ), obtained by linear combination of the experimental spectra of the HS form ( $n_{LS} = 0$ ) and LS form ( $n_{LS} = 1$ ).

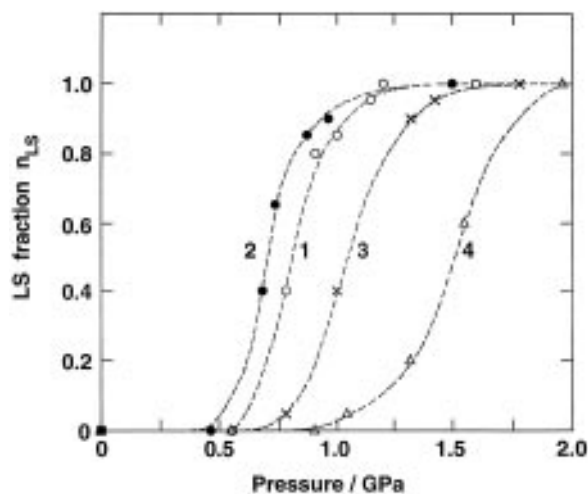


**Figure 8.** Plots of  $n_{LS}$  vs  $P$ , corresponding to the first application of pressure to compounds **1** (O), **2** (●), **3** (x) and **4** (Δ). Dotted lines were drawn for clarity.

that the spin change begins at  $\approx 3.0$  GPa, that  $n_{LS}$  is 0.2 at 4.0 GPa, and that the transformation is already complete ( $n_{LS} = 1$ ) at 8.0 GPa. The characteristic values of pressures obtained for all the compounds are collected in Table 1:  $P_{\text{onset}}^{\uparrow}$  and  $P_{\text{end}}^{\uparrow}$  correspond to the onset and the end of the HS-to-LS conversion upon the first application of pressure and  $P_c$  stands for the pressure at the point of inflexion of the  $n_{LS}$  vs  $P$  plot. Table 1 also gives some other data related to the complexes, which will be detailed below.

Finally, Figure 9 shows the alteration of the spin-crossover behavior of compound **2** when the sample is subjected several times to increasing pressures ( $P^{\uparrow}$ ) and then to decreasing pressures ( $P^{\downarrow}$ ).

## Discussion

**Interpretation of Edge Structures.** Though the  $n_{LS}$  vs  $P$  plots may be obtained without a detailed analysis of the XANES spectra, we recall hereafter the interpretation of the main features of these spectra. They are known to originate in electronic transitions from the 1s core orbital to vacant levels of proper symmetry (the so-called bound states) when photoelectrons are only excited and to the continuum (multiple scattering process) when photoelectrons are ejected with a weak kinetic energy. However, despite the recent progress in this field, a thorough interpretation of the spectra proves always to be difficult,

**Table 1.** Characteristic Values of Pressure<sup>a</sup> and Related Data<sup>b</sup> for Compounds **1–5**

	<b>1</b>	<b>2</b>	<b>3<sup>i</sup></b>	<b>4<sup>k</sup></b>	<b>5</b>
$P_{\text{onset}}^{\uparrow}$ (GPa)	$\sim 0.65$	$\sim 0.45$	$\sim 0.70$	$\sim 0.90$	$\approx 3.0$
$P_{\text{end}}^{\uparrow}$ (GPa)	$\sim 1.30$	$\sim 1.15$	$\sim 1.60$	$\sim 1.90$	$\leq 8.0$
$P_c$ (GPa)	$\sim 0.80$	$\sim 0.65$	$\sim 1.00$	$\sim 1.55$	5–7
$T_c^{\downarrow}$ (K)	176.15 <sup>c</sup>	178.0 <sup>c</sup>	113.5 <sup>j</sup>	106 <sup>j</sup>	—
$T_c^{\uparrow}$ (K)	176.30 <sup>c</sup>	179.5 <sup>c</sup>	116.5 <sup>j</sup>	106 <sup>j</sup>	—
$\Delta V$ (Å <sup>3</sup> )	—	29.7 <sup>e,f</sup>	—	$\sim 26^l$	—
$\Delta V_{\text{sc}}$ (Å <sup>3</sup> )	—	$\sim 18^f$	—	$\approx 6^l$	—
$\Delta S$ (J K <sup>-1</sup> mol <sup>-1</sup> )	48.8 <sup>d</sup>	$\approx 32^g$	56 <sup>j</sup>	37 <sup>j</sup>	—
$k_v^{\text{HS}}$ (10 <sup>-1</sup> GPa <sup>-1</sup> )	—	1.07 <sup>h</sup>	—	0.87 <sup>l</sup>	—
$k_v^{\text{LS}}$ (10 <sup>-1</sup> GPa <sup>-1</sup> )	—	0.82 <sup>h</sup>	—	—	—

<sup>a</sup>  $P_{\text{onset}}^{\uparrow}$  and  $P_{\text{end}}^{\uparrow}$ : pressures corresponding to the onset and the end of the HS-to-LS conversion, respectively.  $P_c$ : transition pressure corresponding to the point of inflexion of the  $n_{LS}$  vs  $P$  curve. <sup>b</sup>  $T_c^{\downarrow}$  and  $T_c^{\uparrow}$ : transition temperatures, corresponding to the points of inflexion of the  $n_{HS}$  vs  $T$  curves in the cooling and the heating modes, respectively.  $\Delta V$ : crystal volume variation (referring to one molecule) between room temperature and 130 K (**2**) or 93 K (**4**), under atmospheric pressure.  $\Delta V_{\text{sc}}$ : crystal volume variation (referring to one molecule) resulting solely from the spin conversion.  $\Delta S$ : entropy variation upon the spin conversion.  $k_v^{\text{HS}}$  and  $k_v^{\text{LS}}$ : volumic compressibility coefficients of the HS and LS forms, respectively. <sup>c</sup> Reference 46. <sup>d</sup> Reference 20. <sup>e</sup> Reference 18. <sup>f</sup> Reference 42. <sup>g</sup> Reference 22. <sup>h</sup> References 11 and 12. <sup>i</sup> The pressure data are related to  $\text{Fe}(\text{py})_2(\text{bpy})(\text{NCS})_2$ , the other data to  $\text{Fe}(\text{py})_2(\text{bpy})(\text{NCS})_2 \cdot 0.25\text{py}$ . <sup>j</sup> Reference 19. <sup>k</sup> The pressure data are related to  $\text{Fe}(\text{py})_2(\text{phen})(\text{NCS})_2$ , the other data to  $\text{Fe}(\text{py})_2(\text{phen})(\text{NCS})_2 \cdot 0.5\text{py}$ . <sup>l</sup> Reference 23.

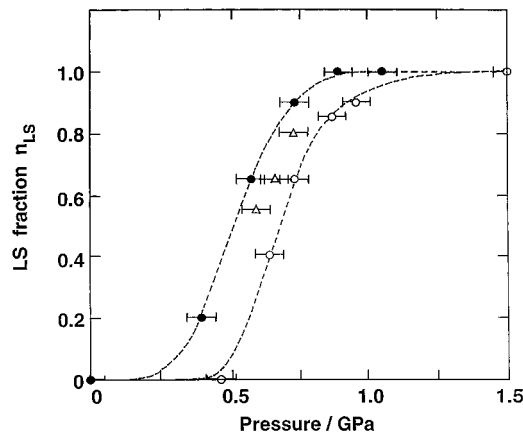


**Figure 9.** Plots of  $n_{LS}$  vs  $P$  obtained for compound **2** upon the first [increasing pressure (O)/decreasing pressure (●)] cycle, and the third application of pressure (Δ).

principally because (i) the ionization energy is not defined by a clear-cut experimental feature, (ii) the excitation process in this energy range is not restricted to one-electron excitations, and (iii)  $x$ -,  $y$ -, and  $z$ -polarized transitions differ in energy and intensity, which renders the transition assignment in an isotropic powder spectrum still more intricate. Moreover, in the case of high-pressure experiments at such a low energy, the experimental resolution is far from being large enough to allow a definitive interpretation of each structure to be given. Nevertheless, a plausible explanation of the main features observed in the spectra of complexes **1–5** can be proposed on the basis of a comparison with other data previously reported.

(1) The weak pre-edge structure observed below 2 eV is assigned to the symmetry-forbidden electric dipolar transitions  $1s \rightarrow (3d \text{ MO}')$ . ( $3d \text{ MO}'$ ) stands for the excited molecular orbital levels centered on the 3d orbitals of the iron absorber, the prime sign recalling that, in the excited state, the molecular levels are relaxed in the core hole. The weak intensity, typical of forbidden transitions, indicates that iron(II) ions are in a quasi-centrosymmetrical position, i.e. in an idealized  $O_h$  symmetry.

In the HS form ( $t_{2g}^4 e_g^2$ ) spectra, the transitions  $1s \rightarrow (t_{2g} MO')$  and  $1s \rightarrow (e_g MO')$  cannot be distinguished: a plausible value of  $\approx 12\,000\text{ cm}^{-1}$  for the ligand-field strength would result in an energy gap of  $\approx 1.5\text{ eV}$ , i.e. on the order of magnitude of the experimental resolution between the two bands. In the LS form ( $t_{2g}^6$ ) spectra, only the transitions to the fully vacant  $e_g$  molecular orbitals can be observed. The corresponding absorptions are higher in energy and narrower than in the HS form spectra.

(2) The white band at  $\approx 16\text{ eV}$  (HS) and  $\approx 18\text{ eV}$  (LS) corresponds to the symmetry-allowed electric dipolar transition  $1s \rightarrow (4p MO')$ . In both the HS and LS forms, the distortion of the coordination core is not sufficiently pronounced for the three components  $1s \rightarrow (4p_{x,y,z} MO')$  to be resolved. The main changes observed for this band upon the HS-to-LS conversion can be safely explained: the  $\approx 2\text{ eV}$  shift to higher energies arises from the shortening of metal-ligand distances through the destabilization of  $4p$  molecular orbitals; the clear decrease in intensity is a consequence of the lesser participation of the  $4p$  metal orbitals resulting from the larger metal-ligand orbital overlap; the absorption narrowing is likely to account for a lowering of the coordination core distortion (evidence was provided for this lower distortion from the crystal structures of the HS and LS forms of **2**<sup>18</sup>). It is worth being underlined that such changes in the white line, which allow K-edge X-ray absorption to be used as a probe for detecting the spin conversion, are due to the structural alteration of the coordination core upon the electronic transition. They are not directly associated with the variation of the electronic configuration of the  $d$  levels.

(3) The various structures observed in the rising part of the edge, whose resolution is somewhat better in the LS form spectra as a consequence of the shift of the white line toward higher energies, might originate from two-electron transitions (shake-down process)<sup>34,36,37</sup> and/or from transitions to  $d-\pi^*$  levels.

(4) The medium intensity absorption at  $\approx 30\text{ eV}$ , i.e. above the ionization energy, is assigned to the multiple scattering of photoelectrons with low kinetic energy.<sup>37,38</sup> This structure is more intense in the LS form spectra than in the HS form spectra, which is likely to be due to closer neighbors and/or to lower Debye-Waller factors.

In all the spectra, the first EXAFS oscillation exhibits several components. This clearly accounts for a distribution of the distances of iron neighbors in both the HS and LS forms of each compound. Upon the HS-to-LS conversion, this band is strongly shifted toward higher energies, as a consequence of the shortening of metal-ligand bond lengths.

It should be noted that, as iron(II) spin crossover ( $t_{2g}^4 e_g^2 \leftrightarrow t_{2g}^6$ ) consists of a two-electron transfer whereas a one-electron transfer is implied in cobalt(II) spin crossover ( $t_{2g}^5 e_g^2 \leftrightarrow t_{2g}^6 e_g^1$ ), which results in a much larger variation of the mean coordination radius in the first case,<sup>39</sup> the related effects on the K-edge X-ray absorption spectra of iron(II) complexes (present work) and cobalt(II) complexes<sup>4</sup> are different. However, in iron(II) species, where the occupancy of both antibonding  $e_g$  orbitals changes with the spin state, the structural alterations are more isotropic and hence the global shape of the spectra is retained. On the other hand, in the case of cobalt(II) species, where only one  $e_g$

orbital is affected by the spin conversion, the spectral modifications reflect the anisotropy of the structural ones.

**How Does Pressure Act?** Before the spin change takes place, the application of pressure, at room temperature, to the HS forms of compounds **1–4** is expected not to significantly alter the coordination cores of these species: metal-ligand bond lengths, in molecular complexes, were predicted to decrease by only  $\approx 10^{-3}\text{ \AA}$  under the effect of a few  $10^{-1}\text{ GPa}$ ,<sup>40</sup> and were effectively found, in compound **2**,<sup>12</sup> to hardly vary under  $1\text{ GPa}$  (vide supra). So, in compounds **1–4**, the shortening of metal-ligand distances should only play a minor role in the starting of the spin change.

Consequently, the main effect of pressure on the HS forms of the four complexes is likely to be a reduction of the unit cell volume, which would result in a lattice strain large enough to induce a transformation to the LS state, of lower volume. The relative variation of volume ( $\Delta V/V$ ) accompanying the thermally-induced spin conversion exhibited by an iron(II) complex is generally of the order of 4–6%, and corresponds to  $\Delta V = 24\text{--}36\text{ \AA}^3$  per metal ion.<sup>41</sup> However, the fact that  $\Delta V$  is the sum of two contributions, viz. the volume change  $\Delta V_{SC}$  only due to the spin crossover and the lattice thermal expansion  $\Delta V_T$ , has to be kept in mind. For **2**,  $\Delta V$  was found to be  $29.7\text{ \AA}^3$  per formula unit ( $\Delta V/V = 5.1\%$ ) in the temperature range 293–130 K,<sup>18</sup>  $\Delta V_{SC}$  being estimated at  $\approx 18\text{ \AA}^3$  for the complete spin conversion.<sup>42</sup> Regarding the spin-crossover species **1**, **3**, and **4**, these parameters could not be determined, either because no suitable crystal was obtained (**1**) or because crystals were damaged upon the spin change (**3** and **4**).

It is well-known that, when a compound exhibits a thermally-induced spin conversion, the stability of its HS and LS forms is ruled out by the Gibbs free energy difference  $\Delta G = G_{HS} - G_{LS} = \Delta H - T\Delta S$ , the enthalpy change  $\Delta H$  and the entropy change  $\Delta S$  being positive. For compounds **1–4**, the spin crossover under  $P_{atm}$  occurs at low temperatures. It follows that, at room temperature,  $T\Delta S$  overbalances  $\Delta H$ , leading to  $\Delta G < 0$ : the HS form is the stable one. As pressure is applied to this form at constant temperature, its effect can be understood by only considering the alteration of

$$\Delta H = H_{HS} - H_{LS} = \Delta E + P\Delta V$$

$\Delta E = E_{HS} - E_{LS}$ , the internal energy change, should little vary since the molecules, as seen above, are expected not to be significantly affected by the moderate pressures required to induce the spin conversion. At  $P_{atm}$ , the term  $P\Delta V$  is small with regard to  $\Delta H$  and, consequently,  $\Delta H \approx \Delta E$ . At increasing pressure this term, which is positive since  $V_{HS} - V_{LS} > 0$ , leads to higher and higher values of  $\Delta H$  and hence to a more and more pronounced stabilization of the LS state. It behaves as the driving force of the spin conversion.

The same reasoning applies to compound **5** in spite of the fact that, at  $P_{atm}$ , the fundamental state of this compound is HS ( $^5T_2$ ) and, consequently,  $\Delta H$  is negative since  $H_{HS}$  is then lower than  $H_{LS}$ . However, in this case, the shortening of metal ligand distances under the effect of the relatively high pressures required to induce the spin conversion ( $P_c \approx 5\text{--}7\text{ GPa}$ ) is likely to be no more negligible and might “help” the HS-to-LS transformation.

**Parameters Influencing the  $n_{LS}$  vs  $P$  Curves.** As can be seen in Table 1, the characteristic values of pressure related to complexes **1–5** depend significantly on the nature of the

(36) Briois, V.; Cartier, C.; Momenteau, M.; Maillard, P.; Zarembowitch, J.; Dartyge, E.; Fontaine, A.; Tourillon, G.; Thuéry, P.; Verdagner, M. *J. Chim. Phys.* **1989**, *86*, 1623.

(37) Cartier, C.; Verdagner, M. *J. Chim. Phys.* **1989**, *86*, 1607.

(38) Briois, V.; Cartier, C.; Sainctavit, P.; Brouder, C.; Flank, A. M. *J. Am. Chem. Soc.* **1995**, *117*, 1019.

(39) Zarembowitch, J. *New J. Chem.* **1992**, *16*, 255.

(40) Hauser, A. *Chem. Phys. Lett.* **1992**, *192*, 65.

(41) König, E. *Prog. Inorg. Chem.* **1987**, *35*, 527.

(42) Real, J. A.; Gallois, B.; Granier, T.; Suez-Panama, F.; Zarembowitch, J. *Inorg. Chem.* **1992**, *31*, 4972.

**Table 2.** Room Temperature  $P_c$  Values Reported for  $\text{Fe}(\text{phen})_2(\text{NCS})_2$ 

reference	crystalline form	$P_c$ (GPa)
Fisher et al. <sup>43</sup>	I	~1.1
Adams et al. <sup>44</sup>	I	~0.8
Pebler <sup>45</sup>	I	~1.35
Usha et al. <sup>14</sup>	I	~0.6
Granier et al. <sup>12</sup>	II	~0.6
present work (1)	I	~0.80
present work (2)	II	~0.65

compounds. In the following, these data will be at first comparatively analyzed. In particular, the  $P_c$  values of the species exhibiting a thermally-induced spin transition will be discussed on the basis of the Clapeyron equation, which can be written  $dP/dT = \Delta S/\Delta V$  ( $\Delta V$ , the crystal volume variation associated with the spin change, is herein denoted  $\Delta V_{\text{SC}}$ ). Even though this equation cannot strictly be applied to the present situations, it suggests that the values of  $\Delta P = P_c - P_{\text{atm}} \approx P_c$  should be correlated with those of  $\Delta T = T_{\text{amb}} - T_c$ ,  $\Delta S$ , and  $\Delta V_{\text{SC}}$ . The available values of  $T_c$ ,  $\Delta S$ , and  $\Delta V_{\text{SC}}$  are given in Table 1.

Let us first consider complexes **1** and **2**. The effect of pressure on the spin state of iron(II) in  $\text{Fe}(\text{phen})_2(\text{NCS})_2$  has been reported in a number of papers.<sup>10–14,43–45</sup> Though most of these studies were published before the polymorphism of this compound was established,<sup>18</sup> we could later on identify the crystalline form examined in each of them as being form I (**1**), on the basis of the synthesis procedure or of the completeness of the thermally-induced HS-to-LS conversion.<sup>18</sup> The most recent data are related to the high-pressure single-crystal X-ray diffraction investigation of form II (**2**), already mentioned.<sup>10–12</sup> The  $P_c$  values resulting from all these studies are collected in Table 2. They differ significantly. However, our data are found to be in close agreement with those of Adams et al.<sup>44</sup> for form I and of Granier et al.<sup>12</sup> for form II.

As visualized in Figure 8, the  $n_{\text{LS}}$  vs  $P$  plot obtained for **1** ( $P_c \sim 0.80$  GPa) is shifted toward higher pressures with regard to that related to **2** ( $P_c \sim 0.65$  GPa). This deviation ( $\Delta P_c/P_c \sim 20\%$ ) cannot be quantitatively correlated with the slightly higher transition temperature of **2**, compared to **1**<sup>46,47</sup> (see Table 1), leading to  $\Delta(T_{\text{amb}} - T_c)/(T_{\text{amb}} - T_c) = 3\%$  at the most. On the other hand, the  $\Delta S$  value we obtained recently for **2** from differential scanning calorimetry ( $\approx 32 \text{ J K}^{-1} \text{ mol}^{-1}$ )<sup>22</sup> is found to be significantly lower than the one determined by Sorai and Seki for **1** ( $48.8 \text{ J K}^{-1} \text{ mol}^{-1}$ ).<sup>20</sup> This difference, of vibrational origin, which is likely to result mainly from the larger mean variation ( $\Delta R$ ) of metal–ligand distances upon the spin conversion in **1** ( $0.24 \text{ \AA}$ ),<sup>33</sup> compared to **2** ( $0.16 \text{ \AA}$ ),<sup>18</sup> might largely account for the relative behaviors of the two polymorphs under the effect of pressure. Finally, regarding the crystal volume variation  $\Delta V_{\text{SC}}$ , for which few data are presently available,<sup>23,42</sup> only a value related to **2** was reported.<sup>42</sup> For lack of data concerning **1**, no conclusion can be drawn on the effect of this parameter on  $P_c$  values. However, since  $\Delta R$  is much higher for **1** than for **2**,  $\Delta V_{\text{SC}}$  can be reasonably assumed to be also larger. As nevertheless  $P_c(\mathbf{1}) > P_c(\mathbf{2})$ , the  $\Delta V_{\text{SC}}$  volumic effect, in the present case, is likely to be overbalanced by the  $\Delta S$  entropic effect.

For compounds **3** and **4**, the trend of  $P_c$  values ( $\sim 1.00$  and  $\sim 1.55$  GPa, respectively) does appear to be inverted with regard

to that of  $T_c$  values ( $\sim 115$  and  $106$  K, respectively). However, as previously,  $\Delta P_c/P_c$  ( $\sim 55\%$ ) is found to be much higher than  $\Delta(T_{\text{amb}} - T_c)/(T_{\text{amb}} - T_c)$  ( $\sim 5\%$ ). Now, comparing  $\Delta S$  values for these species ( $56$  and  $37 \text{ J K}^{-1} \text{ mol}^{-1}$ , respectively) may be somewhat hazardous, because calorimetric measurements were carried out on samples containing pyridine as lattice solvent (see Table 1) and, consequently,  $\Delta S$  might include a nonnegligible contribution resulting from an order–disorder transition of these solvent molecules (which were shown to be disordered at room temperature<sup>19,23</sup>). On the other hand, whatever the trend of  $\Delta S$  may be on passing from **3** to **4** and despite the fact that  $\Delta V_{\text{SC}}$  is still unknown for **3**, the surprisingly low value of this latter parameter found recently for **4**, viz.  $\approx 6 \text{ \AA}^3$  per molecule,<sup>23</sup> might largely be responsible for the relatively high  $P_c$  value related to this complex compared to that obtained for **3**.

Finally, as expected, a high  $P_c$  value ( $5$ – $7$  GPa) was found for compound **5**, which retains the HS state at any temperature under atmospheric pressure. A number of HS complexes were previously reported as presenting the same behavior (as examples, see ref 4 and references therein). This shows that applying pressure is a more efficient way to induce a spin conversion than varying temperature. It should be noted that, for **5**, the spin change can be followed visually, through the diamonds of the high-pressure cell, for it is accompanied by a yellow to deep red change of the sample color.

Both  $\Delta S$  and  $\Delta V_{\text{SC}}$  depend on  $\Delta R$ . However, the effects of a variation of  $\Delta R$  on  $P_c$ , through  $\Delta S$  on the one hand and  $\Delta V_{\text{SC}}$  on the other hand, are opposite, the resulting  $P_c$  value being expected to depend significantly on the crystal structure.

To our knowledge, no structural data were reported so far for **1**. On the contrary, the structures of the HS and LS forms of **2** are well documented.<sup>12,18</sup> In particular, they first allow one to compare the alterations associated with the thermally-induced and pressure-induced HS-to-LS conversions of a given compound. As seen above, these alterations do not significantly differ at the molecular scale, but the unit cell volume under 1 GPa was found to be much lower than the one at 130 K, even after correction for spin-conversion incompleteness (the ratio of molecules retained in the HS state can be estimated at  $\sim 9\%$  under 1 GPa, from the present XANES data, and was reported to be  $\sim 17\%$  at 130 K<sup>18</sup>). Nevertheless, it is worth noting that  $\Delta V_{\text{SC}}$  is independent of the nature of the control parameter.<sup>12,42</sup> Both HS and LS forms crystallize in the same orthorhombic group,  $Pbcn$ , with  $Z = 4$ , and present a strong lattice anisotropy. The crystal packing may be described as sheets of molecules parallel to the  $ab$  plane. Intermolecular contacts shorter than the van der Waals distances were detected. Their number increases on passing from the HS to the LS form, this effect being much more pronounced in the pressure-induced transition than in the thermally-induced one. Intrasheet contacts are more numerous than intersheet ones: in the HS form, for instance, 8 atoms of a given molecule are implied in the former and 4 in the latter. Moreover, the  $\text{Fe}\cdots\text{Fe}$  distances between first neighbors are shorter within a sheet than between two consecutive sheets. These features suggest that the highest compression amplitude should be observed along the  $c$  axis, i.e. perpendicularly to the sheets. The fact that the linear compressibility coefficient  $k_c$  was found to be larger than  $k_a$  and  $k_b$  supports this assumption.<sup>12</sup>

In their HS form, **3**, **4**, and **5** are known to crystallize in the tetragonal space group  $I4_1/a$ , with  $Z = 16$ ,<sup>19</sup> and in the monoclinic space group  $C2/c$ , with  $Z = 8$ <sup>23</sup> and  $Z = 4$ ,<sup>19</sup> respectively. In **3**, the molecules do not lie, as previously, in parallel sheets and the crystal packing does not present any

(43) Fisher, D. C.; Drickamer, H. G. *J. Chem. Phys.* **1971**, *54*, 4825.(44) Adams, D. M.; Long, G. J.; Williams, A. D. *Inorg. Chem.* **1982**, *21*, 1049.(45) Pebler, J. *Inorg. Chem.* **1983**, *22*, 4125.(46) Müller, E. W.; Spiering, H.; Güttlich, P. *Chem. Phys. Lett.* **1982**, *93*, 567.(47) König, E.; Madeja, K. *Inorg. Chem.* **1967**, *6*, 48.

striking feature. The same holds for **5**.<sup>48</sup> Moreover, intermolecular contacts and Fe $\cdots$ Fe distances between first neighbors have not yet been determined for these two species.

In **4**, the number of intermolecular contacts detected was found to be larger than in the HS form of **2**, these contacts implying seven C atoms of the phenanthroline ligand, four C atoms of each pyridine ring and the S atom of one of the NCS<sup>-</sup> groups. In particular, evidence was provided for the existence of  $\pi$ -interactions between two adjoining phenanthroline entities (interplanar distance: 3.43 Å). As, in addition, Fe $\cdots$ Fe distances lie in the range 7.41–10.41 Å (compared to 8.31–11.08 Å in **2**), the HS form of **4** appears to be significantly more compact than that of **2**. The fact that its volumic compressibility coefficient (0.087 GPa<sup>-1</sup>)<sup>23</sup> is lower than that of HS **2** (0.107 GPa<sup>-1</sup>) and is of the same order of magnitude than that of LS **2** (0.082 GPa<sup>-1</sup>)<sup>12</sup> does reflect this situation. Now, crystal lattice stiffness is likely to affect the spin-conversion pressure through  $\Delta V_{\text{contr}}$ , the volume change only resulting from pressure-induced crystal contraction ( $\Delta V = \Delta V_{\text{contr}} + \Delta V_{\text{SC}}$ ). The greater the stiffness, the higher should be the pressure to apply in order that the unit cell be reduced enough for the spin conversion to be triggered. So, the relatively large  $P_c$  value of **4**, compared to that of **2** or **3**, which is likely to be mainly associated with the very low  $\Delta V_{\text{SC}}$  value of this species (vide supra), might also partly result from its rather low compressibility.

Regarding the spin-conversion cooperativity, Figure 8 shows that the slopes of the  $n_{\text{LS}}$  vs  $P$  curves in the vicinity of the point corresponding to  $n_{\text{HS}} = 0.5$  is nearly the same for **1** and **2** on the one hand, and for **3** and **4** on the other hand, the former being steeper than the latter. These characteristics differ from those of the  $n_{\text{HS}}$  vs  $T$  plots (the thermally-induced spin transitions of **1** and **3** are among the sharpest ones ever reported, those of **2** and **4** exhibit a slightly lower cooperativity), which illustrates the basic difference between the effects of increasing the

pressure and decreasing the temperature on a spin-crossover compound. Moreover, the pressure range corresponding to the complete conversion appears to spread all the more as  $P_c$  is higher (see Table 1): it is found to be (in GPa<sup>-1</sup>)  $\sim 0.65$  for **1**,  $\sim 0.70$  for **2**,  $\sim 0.90$  for **3**,  $\sim 1.00$  for **4**, and higher than  $\sim 2$  for **5**. This mainly results from the spin-conversion starting, which gets slower and slower. The origin of such behavior is not clear at the moment.

Finally, let us examine the alteration of the  $n_{\text{LS}}$  vs  $P$  plot, when submitting a complex (here **2**) several times to increasing then to decreasing pressures (see Figure 9). It is similar to that reported for a family of cobalt(II) compounds:<sup>4</sup> upon the first pressure loop, obtaining a given  $n_{\text{LS}}$  fraction requires a pressure significantly lower at  $P\downarrow$  than at  $P\uparrow$  and, on scanning several pressure cycles, the  $P\uparrow$  branch shifts progressively toward the  $P\downarrow$  branch, which remains the same in each loop. The hypothesis suggested previously to account for these effects, viz. the formation of intermolecular hydrogen bonds which might be retained after the first pressure release, must now be rejected since such bonds cannot exist in **2**. Moreover, the assumption of a pressure-induced form II  $\rightarrow$  form I transformation, proposed by Konno et al.<sup>3</sup> in the case of Fe(bpy)<sub>2</sub>(NCS)<sub>2</sub>,<sup>17</sup> cannot apply in the present case as the  $n_{\text{LS}}$  vs  $P$  curve of **1** is shifted toward higher (and not lower) pressures with regard to that of the unperturbed sample of **2**. A plausible explanation for the observed irreversible pressure effect is a progressive decrease of the number of crystal defects (vacancies in particular), which might facilitate the course of the spin conversion.

**Acknowledgment.** We thank Dr. B. Gallois (University of Bordeaux I, Bordeaux, France) and Dr. L. Ouahab (University of Rennes I, Rennes, France) for kindly providing unpublished data on the crystal structures of Fe(py)<sub>2</sub>(phen)(NCS)<sub>2</sub> and Fe(py)<sub>4</sub>(NCS)<sub>2</sub>, respectively.

(48) Ouahab, L. Private communication.